Appl. Phys. B 72, 417–424 (2001) / Digital Object Identifier (DOI) 10.1007/s003400100495

Applied Physics B
Lasers
and Optics

Effects of the linear mismatch and nonlinear asymmetry in the nonlinear coupler

Y. Wang[1,*], **C.K. Lee**[2]

[1] Agilent Technologies, Singapore 1150 Depot Road, Singapore 109673
[2] School of Electrical and Electronic Engineering, Nanyang Technological University, Singapore 639798

Received: 22 August 2000/Published online: 7 February 2001 –

Abstract. Two types of nonlinear couplers exhibit identical coupling behaviors if their corresponding characteristic parameters and linear mismatches are of equal values but opposite signs. Complete power transfer can be attained in a nonlinear coupler when their characteristic parameters, linear mismatch and the input power satisfy an equation. For a mismatch asymmetrical nonlinear coupler, only one input power can lead to the complete power transfer. It leads to some new applications of the nonlinear coupler. The conditions for the stable and unstable equilibrium of the coupler are presented, they depend on the nonlinear asymmetry and linear mismatch. The impact of the nonlinear asymmetry on the switching characteristics is discussed. For a slight asymmetry or mismatch nonlinear coupler, the switching power can be shifted by means of varying the nonlinear symmetry or the linear mismatch while the switching features remain nearly unchanged. The impact of the mismatch on the operation of the coupler can be counteracted by the asymmetry of the nonlinearity. When the nonlinear asymmetry is high, the nonlinear coupler exhibits good limiting characteristics but not switching characteristics.

PACS: 42.65.Wi; 42.81.Qb; 42.82.Et

The nonlinear directional coupler has been investigated extensively owing to its potential applications in all-optical signal processing since its operation characteristics were first discussed by Jensen [1–22]. Many applications [1–7] have been proposed by means of its power-dependent transmission characteristics. Self-switching in the nonlinear fiber coupler and nonlinear waveguide directional coupler have been demonstrated experimentally [8–10]. The theoretical studies on the nonlinear coupler reported so far have included: symmetrical nonlinear coupler composed of two identical nonlinear waveguides with or without nonlinear saturation [11–14], asymmetrical nonlinear couplers composed of two waveguides with different nonlinear coefficient or different propagating constants [15–18]. The nonlinear coupler composed of one self-focusing waveguide and one self-defocusing waveguide [19] was also examined. By employing the phase portrait, the effect of the linear and nonlinear mismatch on the coupling behavior has also been examined, where only the nonlinear coupler composed of the two self-focusing cores was discussed [16]. Trillo and Wabnitz examined the nonlinear nonreciprocity caused by the linear mismatch [15], where the solutions for the single-input asymmetrical mismatch were presented in a general form, but they are difficult to use. Although a complete power transfer has been observed numerically in the coupler consisting of one linear core and one nonlinear core [17], the general conditions for the complete power transfer in a coupler with arbitrary mismatch and asymmetry remain unknown. By taking advantage of the pitchfork behavior near the unstable equilibrium of the coupler, many useful and interesting applications of the symmetry-match nonlinear coupler have been presented [2, 13], but the general conditions for the unstable equilibrium have not been presented. Daino et al. [20, 21] were the first to investigate the nonlinear coupling behavior by utilizing the phase portrait. They introduced three first-order equations to describe the nonlinear coupling and a 3-dimensional portrait is employed. In fact, a conservative nonlinear coupling system is a 2-dimensional differential system. The coefficients of these two differential equations are variable and are dependent on the initial inputs of the coupler. Consequently, each nonlinear coupling system actually includes an infinite 2-dimensional differential subsystem. To discover the general characteristics, a larger number of simulations are needed. We found that there is only one or a pair of trajectories in the portrait where the two conservation qualities of the coupling system are given. It makes the analysis of the nonlinear simpler. The knowledge of the stable and unstable equilibrium facilitates understanding of the general characteristics of the coupler by means of fewer simulations. Atai et al. [16] tried to obtain the input conditions associated with the equilibrium but

*Corresponding author.
(Fax: +65-79-7933318, E-mail: you.fa_wang@sg.exch.agilent.com)

their results were incorrect. Here the input conditions for the equilibrium are presented.

In this paper, the coupling behavior in the nonlinear coupler composed of two cores with arbitrary linear and nonlinear mismatch is investigated analytically. The coupler composed of two self-focusing cores with $P_{c1} > 0$, $P_{c2} > 0$ and δ exhibits behavior identical to the coupler composed of two self-defocusing cores with $P'_{c1} = -P_{c1}$, $P'_{c2} = -P_{c2}$ and $\delta' = -\delta$. The coupler composed of one self-focusing core and one defocusing-core with $P_{c1} > 0$, $P_{c2} < 0$ and δ also exhibits the same coupling behaviors as the coupler with $P'_{c1} = -P_{c1}$, $P'_{c2} = -P_{c2}$ and $\delta' = -\delta$ when they are both excited from either waveguide 1 or 2. Analytical solutions expressed in terms of elliptical functions for the nonlinear coupler are presented. Utilizing the analytical solutions and the portraits, we also show that the coupler is at an equilibrium state when the module of the elliptical function is 1. Complete transfer of power in the mismatched asymmetrical nonlinear coupler is obtained when the characteristics parameters P_{c1}, P_{c2}, δ and the input power P_t satisfy a special condition. Except for the linear matched symmetrical nonlinear coupler, there is only one input power that can lead to the complete power transfer. This feature suggested a band-pass power-filter and electro-optical switch with an ultralow switching-voltage. Nonreciprocity in the coupler caused by the nonlinear asymmetry is also observed. For a slight mismatch or asymmetry coupler, the switching power of the coupler can be shifted by varying the asymmetry or the mismatch while the switching features remain nearly unchanged, and the operating characteristics are more sensitive to the linear mismatch compared with the nonlinear asymmetry. When the nonlinear asymmetry is high, the coupler is more suitable for application as a limiter but not for a switching.

1 Theory

The coupled equations for the slowly varying mode amplitudes a_1 and a_2 of the two single-mode waveguides can be expressed as [1, 11, 12]

$$-j\frac{\mathrm{d}a_i}{\mathrm{d}z} = \beta_i a_i + C a_{3-i} + \gamma_i |a_i|^2 a_i, \tag{1}$$

where i =1,2. a_1 and a_2 indicate the complex amplitudes of the modes in waveguides 1 and 2, respectively. C and γ_i (i =1,2) stand for the linear coupling coefficient and the nonlinear self-coupling coefficient, respectively, as defined as (2) and (3) in [11]. The nonlinear self-coupling coefficient γ_i is dependent on both the Kerr coefficient n_2 of the material and the effective core area of the waveguide [23]. To analyze (1), we make the following substitutions:

$$a_i = \sqrt{P_c}\, A_i \, \exp\left(jz(\beta_1+\beta_2)/2 + j\phi_i(z)\right), \tag{2}$$

where P_c is a normalized constant. A_i and ϕ_i (i =1,2) are the real functions of z. ϕ_1 and ϕ_2, which are induced by the nonlinear coupling, are the nonlinear phases of beams propagating in waveguides 1 and 2, respectively.

Substituting (2) into (1), the differential equation for the power propagating in waveguide can be obtained:

$$\left(\frac{\mathrm{d}P_i}{\mathrm{d}Z}\right)^2 = P_1 P_2 - \left(\Gamma - \delta P_1 - \frac{P_c}{P_{c1}} P_1^2 - \frac{P_c}{P_{c2}} P_2^2\right)^2, \tag{3}$$

where $P_{ci} = C/4\gamma_i$ (i =1,2) are the characteristics parameters [1] for waveguides 1 and 2. $\delta = \frac{(\beta_1+\beta_2)}{2C}$ is the linear mismatch between the two waveguides. $Z = 2Cz$ is the normalized longitudinal coordinate z. $P_1 = A_1^2(Z)$ and $P_2 = A_2^2(Z)$ are the normalized optical powers in waveguides 1 and 2, respectively. $P_t = P_1 + P_2$ is the total input power. Γ is another conservation quantity of the nonlinear coupling systems and can be determined by the initial inputs.

$$\Gamma = \sqrt{P_{10} P_{20}} \cos\varphi_0 + \delta P_{10} + \frac{P_c}{P_{c1}} P_{10}^2 - \frac{P_c}{P_{c2}} P_{20}^2, \tag{4}$$

where $P_{i0} = P_i(0)$, i =1,2. φ_0 is the initial phase difference.

It is apparent that power evolution is dependent on the characteristic parameters P_{c1}, P_{c2}, the linear mismatch δ and the initial inputs. According to (3) and (4), the nonlinear coupler with characteristic parameters P_{c1}, P_{c2} and δ excited by two beams with phase difference φ_0 obeys the same power-evolution equations as the coupler with $P'_{c1} = -P_{c1}$, $P'_{c2} = -P_{c2}$ and $\delta' = -\delta$ excited by two beams with phase difference $\varphi'_0 = \varphi_0 + \pi$. Therefore, the coupler composed of two self-defocusing cores exhibits the same characteristics as the corresponding coupler composed of two self-defocusing cores.

In the case of single-input excitation, assuming $P_{20} = 0$ and $P_{10} = P_t$, then we have $\Gamma = \delta P_t + \frac{P_c}{P_{c1}} P_t^2$, and (3) can be reduced to

$$\left(\frac{\mathrm{d}P_2}{\mathrm{d}Z}\right)^2 = P_1 P_2 - P_2^2(\eta - \xi P_2)^2. \tag{5}$$

where $\eta = \delta + 2\frac{P_c}{P_{c1}} P_t$ and $\xi = \frac{P_c}{P_{c1}} + \frac{P_c}{P_{c2}}$.

According to (5), the nonlinear coupler composed of one self-focusing core and one self-defocusing core with $P_{c1} > 0$, $P_{c2} < 0$ and δ also obeys the same power-evolution equations as the coupler with $P'_{c1} = -P_{c1} < 0$, $P'_{c2} = -P_{c2} > 0$ and $\delta' = -\delta$ when both are excited from either waveguide 1 or 2 . Thus, the coupling behavior of the nonlinear coupler excited from the self-defocusing core can be obtained directly from the corresponding coupler excited from the self-focusing core. Therefore, we only need to discuss two cases: the coupler composed of two self-focusing cores and, the coupler composed of one self-focusing and one self-defocusing core excited from the self-focusing core.

1.1 $\xi = 0$, namely $P_{c1} = -P_{c2}$

The coupler consists of one self-focusing core and one self-defocusing core. The power evolution along the coupler can be obtained by solving (5) and the results are:

$$P_2(Z) = \frac{P_t}{1+\eta^2} \sin^2\left(\frac{\sqrt{1+\eta^2}}{2} Z\right) \tag{6a}$$

$$P_1(Z) = P_t - \frac{P_t}{1+\eta^2} \sin^2\left(\frac{\sqrt{1+\eta^2}}{2} Z\right). \tag{6b}$$

The nonlinear coupler operates as a linear coupler with an additional mismatch proportional to the input power, as predicted in [15].

1.2 $\xi \neq 0$

(5) can be rewritten as

$$\left(\frac{\mathrm{d}P_2}{\mathrm{d}Z'}\right)^2 = -P_2\left(P_2^3 - \frac{2\eta}{\xi}P_2^2 + \frac{1+\eta^2}{\xi^2}P_2 - \frac{P_t}{\xi^2}\right), \tag{7}$$

where $Z' = |\xi|Z$.

Equation (7) integrates as an elliptical integral. In order to calculate the integral of (7), it is necessary to solve the following cubic equation:

$$P_2^3 - \frac{2\eta}{\xi}P_2^2 + \frac{1+\eta^2}{\xi^2}P_2 - \frac{P_t}{\xi^2} = 0. \tag{8}$$

Let $h = \frac{3-\eta^2}{9\xi^2}$ and $g = \frac{1}{54\xi^3}(2\eta^3 + 18\eta - 27\xi P_t)$. There are two cases to be considered: (i) (8) has three real roots when $h^3 + g^2 \leq 0$. (ii) (8) has one real root and two conjugate complex roots when $h^3 + g^2 > 0$.

1.2.1 $h^3 + g^2 \leq 0$. When $h^3 + g^2 \leq 0$, we have $h \leq 0$, consequently $\eta \geq \sqrt{3}$ or $\eta \geq -\sqrt{3}$. When $h \neq 0$, (8) has three real roots $y_1 > y_2 > y_3$, and the roots are $y_n = 2\sqrt{-h}\cos\left(\frac{\theta+2(4-n)\pi}{3}\right) + \frac{2\eta}{3\xi}$, $(n = 1.2.3)$ where $\theta = \cos^{-1}(-g/\sqrt{-h^3})$ and $h < 0$. The solution to (7) can be written as the following [22]:

$$P_2 = \frac{y_1 y_3 sn^2(R\xi Z, k)}{(y_1 - y_3) + y_3 sn^2(R\xi Z, k)}, \tag{9a}$$

$$k^2 = \frac{(y_1 - y_2)y_3}{(y_1 - y_3)y_2}, \tag{9b}$$

where $R = \frac{\sqrt{(y_1-y_3)y_2}}{2}$ and $P_2 \leq y_3$.

For $h = 0$, we have $h = 0$ and $g = 0$. This leads to $\eta = \sqrt{3}$ and $P_t = 8\sqrt{3}/9\xi$ or $\eta = -\sqrt{3}$ and $P_t = -8\sqrt{3}/9\xi$. Now the three real roots of (8) are $y_1 = y_2 = y_3 = 2\eta/3\xi$. Equation (7) can be reduced to

$$\left(\frac{\mathrm{d}P_2}{\mathrm{d}Z'}\right)^2 = -P_2\left(P_2 - \frac{2\eta}{3\xi}\right)^3. \tag{10}$$

By solving (10), we have

$$P_2 = 3P_t\frac{Z_2}{4(3+Z^2)}. \tag{11}$$

Apparently, the powers in the two waveguides do not interchange periodically. The power in waveguide 2, namely P_2, increases with the increase of the coupling length. P_2 approaches $3P_t/4$ when $Z \to \infty$. Obviously, (11) can not be directly derived from (9). Considering the case of $y_1 \to y_2$ and $y_1 \to y_3$, according to (9) and the definition of elliptic function we have the approximations $R \to 0$ and $sn(R\xi Z) \to R\xi Z$ then Eq.(9) reduces to $P_2 = y_1\frac{y_2 y_3 Z'^2}{4+y_2 y_3 Z'^2}$. Let $y_1 = y_2 = y_3 = 2\eta/3\xi$, P_2 reduces to (11). Therefore, is continuous according to variable in the neighborhood of $|P_t| = 8\sqrt{3}/9\xi$.

1.2.2 $h^3 + g^2 > 0$. In this case (8) has one real root y_1 and two complex roots, and the real root is $y_1 = u + v + 2\eta/3\xi$, where $u = (-g + \sqrt{h^3 + g^2})^{\frac{1}{3}}$ and $v = (-g - \sqrt{h^3 + g^2})^{\frac{1}{3}}$.

The solution for (7) can be written as [22]:

$$P_2 = y_1 q\frac{2 - cn(R\xi Z, k)}{R^2 + q + (R^2 - q)cn(R\xi Z, k)}, \tag{12a}$$

$$k^2 = \frac{1}{2} - \frac{2q + y_1(y_1 - 2\eta/\xi)}{4R^2}, \tag{12b}$$

where $q = \frac{(y_1-2\eta/\xi)^2+3(u-v)^2}{4}$, $R^4 = q(q + 2y_1(y_1 - \eta/\xi))$.

According to (12), we have $P_2 \leq y_1$, $P_2 = y_1$ and when $cn(R\xi Z, k) = -1$. We also have $y_1 = P_t$ when $\eta = P_t\xi$ and $\eta < 2$. Thus, complete power transfer can be attained when $\eta = P_t\xi < 2$. In this case we have $y_1 = P_t = \eta/\xi$, $R^2 = q$, $q = \frac{1}{\xi^2} + P_t^2$ and $k^2 = \frac{\xi^2 P_t^2}{4(1+\xi^2 P_t^2)}$, and thus (12) is reduced to

$$P_2 = \frac{P_t}{2}(1 - cn(R\xi Z, k)), \tag{13}$$

It is apparent that complete transfer of power can be obtained. The conditions for the complete power transfer can be rewritten as

$$\delta = P_t(\frac{P_c}{P_{c2}} - \frac{P_c}{P_{c1}}) \text{ and } \delta + 2\frac{P_c}{P_{c1}}P_t < 2. \tag{14}$$

When linear mismatch and input power satisfy the above conditions, the two waveguides become phase-matched through the power-induced refractive index change. Complete straight-through state and bar state can be obtained. The following observations can be seen from (14):

(i) For the case of the matched and symmetric coupler, which includes the coupler composed of two self-focusing cores and the coupler composed of two self-defocusing cores, complete power transfer can be obtained when $P_t < P_{c1}/P_c$ as expected from previous results.
(ii) For both linear mismatched symmetrical coupler and the linear mismatched asymmetric coupler, no complete power transfer can be attained.
(iii) For linear mismatched asymmetrical, only one value of P_t can satisfy (14), that is, the complete power transfer can be obtained for only one input power. Thus, the coupler exhibits the band-pass power-filter characteristics.
(iv) Complete power transfer can also be obtained in the coupler composed of one linear waveguide and one nonlinear waveguide. Let us assume waveguide 1 is nonlinear and waveguide 2 is linear, namely $P_{c2} \to \infty$. Whether the coupler is excited from the linear waveguide or the nonlinear waveguide, when $\delta = -P_t$ and $P_t < 2$ where P_t is normalized to P_{c1}, complete power transfer can be obtained. Apparently, only when the propagating constant of the linear waveguide is larger than that of the self-focusing waveguide, can complete power transfer be attained.

According to (9b) and (12b), we have $k = 1$ only when the following equation is satisfied

$$g + \sqrt{-h^3} = 0. \tag{15}$$

In this case we have $\theta = 0$ and thus $y_2 = y_3$. Equation (9) reduces to

$$P_2 = \frac{y_1 y_3 (1 - \sec h^2(R\xi Z))}{y_1 - y_3 \sec h^2(R\xi Z)}. \tag{16}$$

When $Z \to \infty$, we have $P_2 = y_3 = 2\eta/3\xi + \sqrt{-h}$.

In the following section, we will show that (15) is also the condition of the unstable equilibrium of the coupler. Many interesting applications of the matched symmetrical nonlinear coupler have been presented taking the pitchfork behavior near the unstable equilibrium.

2 Numerical results

2.1 Spatial instabilities and its condition

The phase-space portrait is useful for obtaining a better understanding of the coupling behavior and facilitating exploitation of the application of the nonlinear coupler especially when the analytical solution is impossible or cumbersome. In order to investigate the power evolution, (1) can be expressed in terms of real variables $S_1 = (|a_1|^2 - |a_2|^2)/P_c = P_1 - P_2$, $S_2 = (a_1 a_2^* + a_1^* a_2)/P_c$, $S_3 = (ia_1^* a_2 - ia_1 a_2^*)/P_c$, and the equations become [16, 20, 21]

$$\frac{dS_1}{dZ} = S_3, \tag{17a}$$

$$\frac{dS_2}{dZ} = -(\delta + \frac{P_c P_t}{P_{c1}} - \frac{P_c P_t}{P_{c2}} + \xi S_1) S_3, \tag{17b}$$

$$\frac{dS_3}{dZ} = -S_1 + (\delta + \frac{P_c P_t}{P_{c1}} - \frac{P_c P_t}{P_{c2}} + \xi S_1) S_2. \tag{17c}$$

For a conservative coupled system, (17) is a two-dimensional differential system since $S_1^2 + S_2^2 + S_3^2 = P_t^2$. Therefore, a two-dimensional phase portrait, not a three-dimensional portrait should be adopted. By using (17a) and (17b) to eliminate S_2, (17c) becomes

$$\frac{dS_3}{dZ} = -S_1 + \left(\delta + \frac{P_c P_t}{P_{c1}} - \frac{P_c P_t}{P_{c2}} + \xi S_1\right) \left[T - \left(\delta + \frac{P_c P_t}{P_{c1}} - \frac{P_c P_t}{P_{c2}}\right) S_2 - \frac{\xi}{2} S_1^2\right], \tag{18}$$

where T is a constant which can be determined by the initial inputs, and

$$T = S_2(0) + \left(\delta + \frac{P_c P_t}{P_{c1}} - \frac{P_c P_t}{P_{c2}}\right) S_1(0) - \frac{\xi}{2} S_1^2(0). \tag{19}$$

Now, the power coupling behavior in the nonlinear coupler can be described by the two first-order coupled differential equations, namely (17a) and (18). Obviously, (18) is a variable coefficient differential equation, and the coefficients are dependent on the initial inputs P_t and T. For a set of given values of P_t and T, (17a) and (18) defined a 2-dimensional differential subsystem. Therefore, a nonlinear coupling system described by (17a) and (18) includes infinite 2-dimensional differential subsystems. Each subsystem has an unique phase portrait. Therefore, to get the general characteristics of a nonlinear coupler, a great number of portraits are needed. Fortunately, there is only one or a pair of trajectories in the portrait of each subsystem featured by P_t and T. Figure 1 shows the portraits of two subsystems of the nonlinear coupling system with $\delta = -0.3$ and $a = 1.2$. Figure 1a corresponds to the coupling subsystem with $P_t = 1.4$ and $T = 1.334$, and Fig. 1b corresponds to the coupling subsystem with $P_t = 1.6$ and $T = 1.334$. Obviously, these two subsystems are different since (18) is also a function of P_t. For a given set of P_t and T, initial inputs $S_1(0)$ and $S_3(0)$ can be chosen by (19) and the equality $S_1^2 + S_2^2 + S_3^2 = P_t^2$. Clearly, the choices of the initial inputs are infinite, however, there is only one or a pair of trajectories as shown in Fig. 1. It makes the analysis of the nonlinear coupler by means of a portrait simpler.

For a symmetrical nonlinear coupler (i.e. $P_{c1} = P_{c2}$), the coefficients of (18) are only dependent on T. Each given value of T defines a subsystem. Figure 2 shows the portrait of a subsystem featured by $T = 0.88$ of the nonlinear coupled system with $\delta = -0.3$ and $a = 1$. Each trajectory corresponds to a special P_t in Fig. 2 since there is only one or a pair of trajectories in the portrait for each set of values of P_t and T. As can be seen from Fig. 2, the nonlinear coupler has two operating modes: mode 1 and mode 2. For mode 1, complete power transfer is permitted, whereas for mode 2 most of the input power remains in the excited core. A separatrix trajectory divides the trajectories corresponding to mode 1 from the trajectories corresponding to mode 2.

In the portrait, a point (S_1,S_3) where the phase velocity is zero, namely $\frac{dS_{1,3}}{dZ} = 0$, is named a fixed point and represents a system in equilibrium. Obviously, point A in Fig. 2 is a fixed point; it is a hyperbolic point which represents an unstable equilibrium state. It implies that the nonlinear

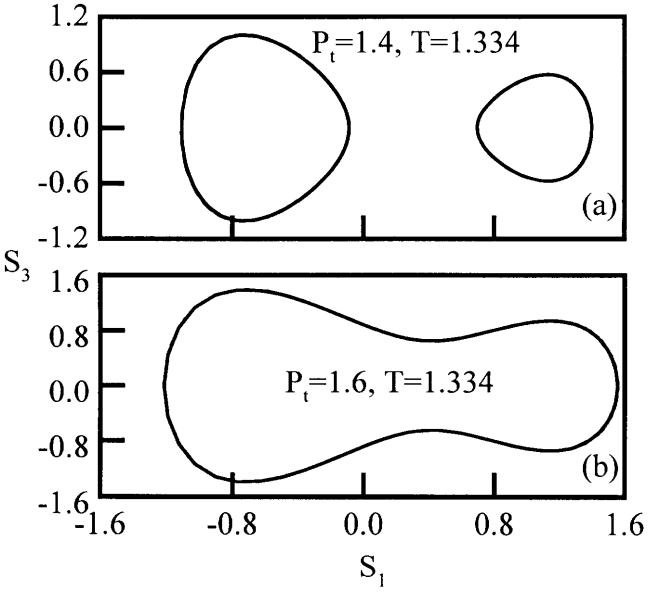

Fig. 1. Portraits of two subsystems of the nonlinear coupling system with $\delta = -0.3$ and $P_{c1}/P_{c2} = 1.2$

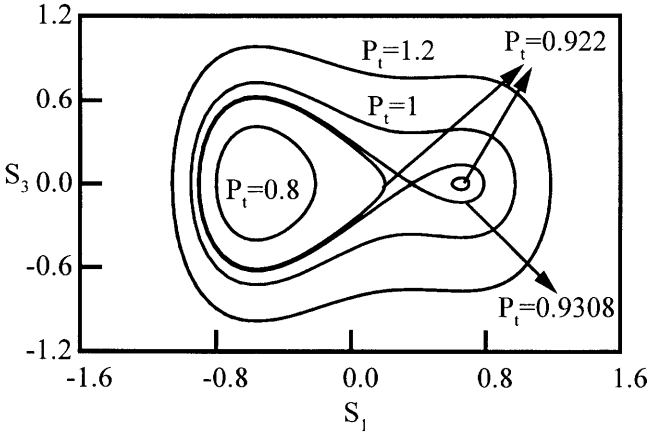

Fig. 2. Portrait of a $T = 0.88$ subsystem of the nonlinear coupled system with $\delta = -0.3$ and $P_{c1} = P_{c2}$

coupler is subject to spatial instabilities for the corresponding P_t and T. The fixed point can show us the structure of the phase flow in its neighborhood and together they often give us a good indication of the nature of the flow in the phase space. Without the knowledge of the fixed points, it is not convenient to investigate the coupling characteristics by means of the portrait. Fortunately, the fixed point is related to the input conditions and it can be obtained by the following equations

$$\frac{\mathrm{d}S_1}{\mathrm{d}Z} = 0 \text{ and } \frac{\mathrm{d}^2 S_1}{\mathrm{d}Z^2} = 0. \tag{20a}$$

Similarly,

$$\frac{\mathrm{d}P_2}{\mathrm{d}Z} = 0 \text{ and } \frac{\mathrm{d}^2 P_2}{\mathrm{d}Z^2} = 0. \tag{20b}$$

By using (20b), the input conditions corresponding fixed point can be obtained. For the case of the single-input nonlinear coupler, by using (7) and (20b) we have

$$X^3 + 3hX + 2g = 0 \tag{21a}$$

$$X^2 + h = 0 \tag{21b}$$

where $P_2 = X + 2\eta/3\xi$, $h = \frac{3-\eta^2}{9\xi^2}$ and $g = \frac{1}{54\xi^3}(2\eta^3 + 18\eta - 27\xi P_t)$. Equation (21) include two one-dimensional equations. By solving (21), we have

$$g + \sqrt{-h^3} = 0 \text{ when } X = -\sqrt{-h}, \tag{22a}$$

$$g - \sqrt{-h^3} = 0 \text{ when } X = \sqrt{-h}, \tag{22b}$$

(22b) should be discarded. In the case of $g - \sqrt{-h^3} = 0$, we have $P_2 \le 2\eta/3\xi - 2\sqrt{-h}$, but we have $P_2 = 2\eta/3\xi + 2\sqrt{-h}$ when $X = \sqrt{-h}$. Obviously, the conditions for the equilibrium are just the conditions for the module of the elliptical functions to equal 1 (see (15)). It also implies that there is no stable equilibrium in the single-input nonlinear coupler. In the case of matched symmetrical nonlinear, the equilibrium conditions, namely (15) or (22a) reduce to $P_t = 1$ as predicted in [2].

2.2 Influence of the asymmetry and linear mismatch on the switching characteristics

In practice, a linear matched and nonlinear symmetrical coupler is difficult to fabricate, hence it is useful to discuss the influence of the mismatch and asymmetry on the operating characteristics. Figure 3 shows the influence of the nonlinear asymmetry on the switching characteristics of the linear matched coupler with single-input excitation.

As shown in Fig. 3, the switching power increases with the increase of the nonlinear asymmetry. With the increase of the nonlinear asymmetry, the switching characteristic curves rise slightly whereas the extinction ratio decreases.

Figure 4 shows the influence of the linear mismatch δ on the switching characteristics of the symmetrical couplers with single-input excitation. It is obvious that the switching power increases with the decrease of the linear mismatch while the switching characteristic remains nearly unchanged. Both Figs. 3 and 4 show that slight linear mismatch and

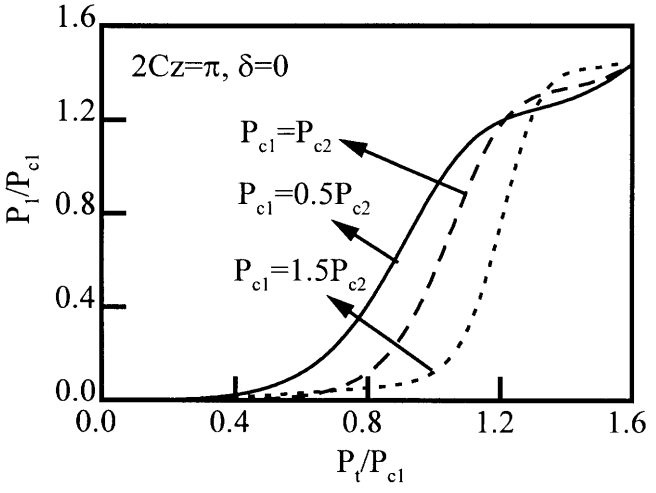

Fig. 3. The influence of the nonlinear asymmetry on the switching characteristic curves, where all the power is launched into waveguide 1. The normalized coupling length $2Cz = \pi$ and the linear mismatch $\delta = 0$

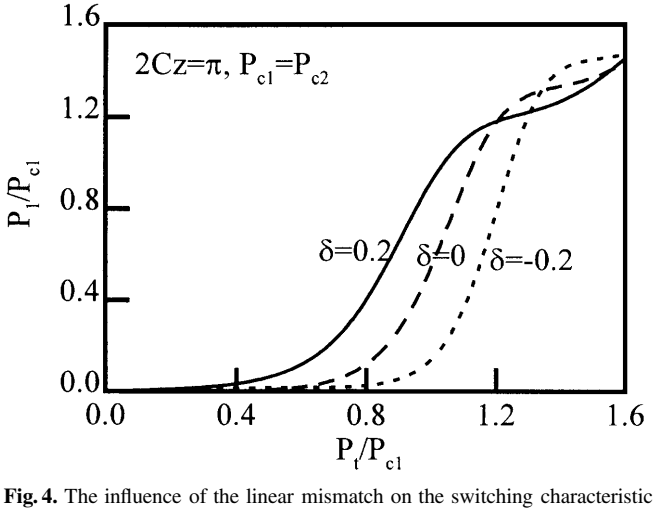

Fig. 4. The influence of the linear mismatch on the switching characteristic curves, where all the power is launched into waveguide 1. The normalized coupling length $Z = \pi$ and $P_{c1} = P_{c2}$

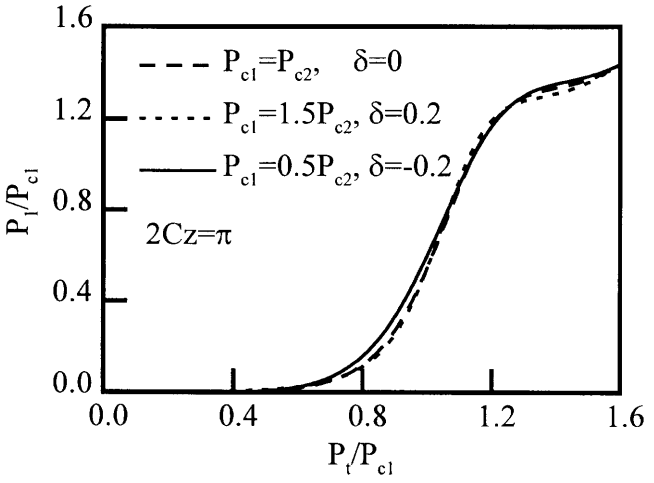

Fig. 5. Some typical switching characteristics of nonlinear couplers, where all the power is launched into waveguide 1 and the normalized coupling length $2Cz = \pi$

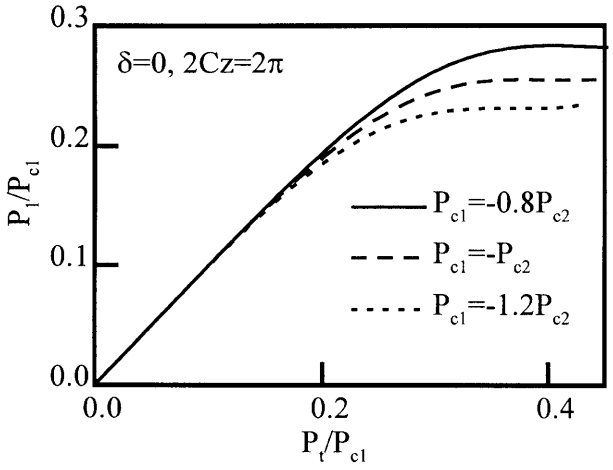

Fig. 6. Limiting characteristics of the coupler composed of one self-focusing core and one self-defocusing core. The normalized coupling length $Z = 2\pi$ and the linear mismatch $\delta = 0$

nonlinear asymmetry will not markedly degrade the switching characteristics, and that the impact of the linear mismatch is interchangeable with that of the nonlinear asymmetry. The comparison between Figs. 3 and 4 also shows that appropriate choice of the linear mismatch and nonlinear asymmetry may lead to the characteristics of the linear matched symmetrical nonlinear coupler. Figure 5 shows the switching characteristics for three couplers with single-input excitation.

It is apparent that the two couplers with different linear mismatch and nonlinear asymmetry can result in the same switching characteristics as shown as the dotted line and the dashed line. Although both the linear mismatch and the nonlinear asymmetry cause the incomplete or deteriorated power switching, the switching characteristics of an ideal nonlinear coupler are possible to obtain by a proper combination of a linear mismatch and a nonlinear asymmetry.

2.3 The influence of the asymmetry on the limiting characteristics

The nonlinear coupler composed one self-focusing core and one self-defocusing core can be used as an optical limiter. Figure 6 shows the straight-through output power of a coupler composed of one focusing core and one defocusing core as a function of the input power in the case of single-input excitation.

It can be seen from Fig. 6 that the output power increases linearly with the increase of the input power when $P_t \leq 0.22P_c$, whereas it remains nearly unchanged when $0.22P_c < P_t \leq 0.4P_c$. It means that the coupler composed of one focusing core and one defocusing core with single-input exhibits limiting characteristics. It is different from the limiting characteristics of the cascaded nonlinear couplers, where the output power is 0 when the input power is less than the characteristic power [5].

It can also be seen that the limiting level increases with the decrease of the nonlinear asymmetry while the limiting characteristic remains unchanged. The limiting characteristics are sensitive to the linear mismatch.

2.4 Nonreciprocity in the nonlinear coupler caused by the asymmetry

Nonreciprocity caused by the linear mismatch has been observed by Trillo and Wabnitz in a symmetrical nonlinear coupler [15]. There is nearly no power coupling between the two waveguides when the power is initially launched into the slow waveguide, whereas for some power there is nearly complete power transfer between the two waveguides when the power is initially into the fast waveguide. Here we will examine the influence of the nonlinear asymmetry on the coupling behavior. Figure 7 shows the evolution of the output power along the coupler. It is obvious that most of the power can be transferred from one waveguide to another one when it is excited from the core with low nonlinear coupling coefficient, whereas only a small part of power can be transferred from one to another when it is excited from the core with high nonlinear coupling coefficient except for the very low

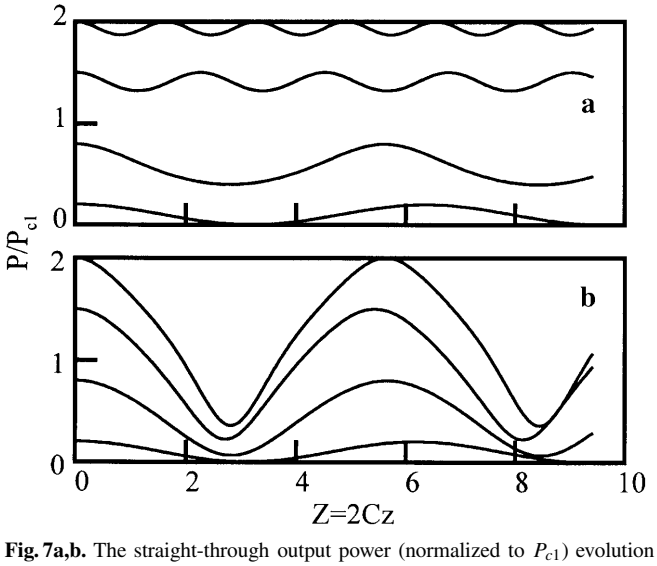

Fig. 7a,b. The straight-through output power (normalized to P_{c1}) evolution along the coupler, where $P_{c2} = 2P_{c1}$ and $\delta = 0$. **a** Power is initially launched into waveguide 1. **b** Power is launched into waveguide 2

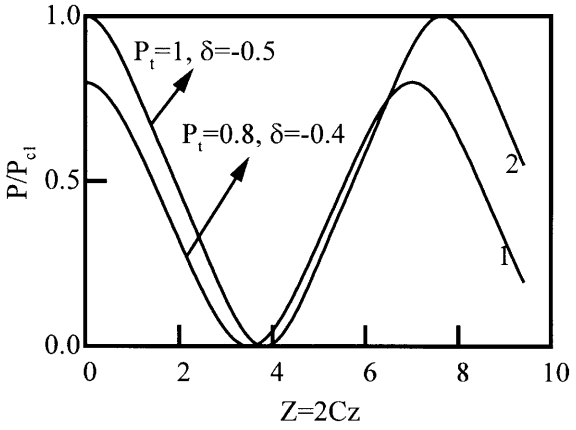

Fig. 8. The straight-through output power evolution along the coupler when $\delta = P_t[(P_{c1}/P_{c2}) - 1]$ and $P_{c1} = 0.5P_{c2}$, the coupler was excited from either core 1 or 2

input power. Additionally, the coupling periodicity is nearly independent of the input power when the power is initially launched into the core with weak nonlinear coefficient. For both the two input cases there are no nonperiodic curves in Fig. 7 since in this case the modules of the elliptical function can not be 1.

However, when (14) is satisfied, the linear mismatched nonlinear asymmetrical coupler exhibits the reciprocity. Figure 8 shows the power evolution along the mismatch asymmetrical coupler. It can be seen that the coupler exhibits the reciprocity when $\delta = P_t(\frac{P_c}{P_{c2}} - \frac{P_c}{P_{c1}})$. If $\delta + 2\frac{P_c}{P_{c1}}P_t < 2$, the complete power transfer can be obtained as shown as the curves 1 and 2.

2.5 Band-pass power-filter

Band-pass power-filter has been observed in the coupler composed of one nonlinear core and one linear core when the nonlinear core is excited [17]. In fact, according to (14) the band-pass power-filter can be realized in a coupler composed of two self-defocusing cores, two self-focusing cores or one self-focusing core and one self-defocusing core. Figure 9 shows the input–output characteristic curves of a mismatch asymmetrical nonlinear coupler when all the power is launched into waveguide 1. It is apparent that most of the power transfers from one waveguide to another in the neighborhood of $P_t = 0.5$, whereas when the input is somewhat lower or higher than $P_t = 0.5$, most of the power remains in the input waveguide as shown as Fig. 9a. When the linear mismatch changes to 1.04, most of the power will remain in the input waveguide as shown in Fig. 9b. Comparison of Figs. 9a and 9b shows that the variations of the mismatch δ of 0.04 can switch the power between the two waveguide when the beam with power $P_t = 0.5$ is launched into waveguide 1 of the nonlinear coupler. The mismatch can be produced by means of voltages. It implies that it is possible for the electro-optical switch with ultralow switching-voltage.

2.6 Limiter

In Sect. 1, we have shown that the impact of the linear mismatch and the nonlinear asymmetry is not obvious, and the

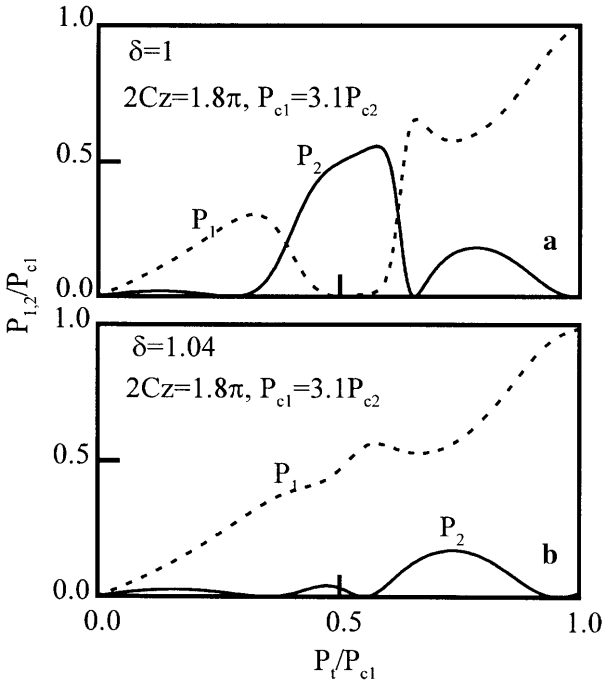

Fig. 9a,b. Input-output characteristics for a nonlinear coupler. The normalized coupling length $Z = 2\pi$ and $P_{c2} = 3.1P_{c1}$. **a** The linear mismatch $\delta = 1$. **b** $\delta = 1.04$

coupler exhibits good switching characteristics when the mismatch and the asymmetry are small. However, the nonlinear coupler does not exhibit the switching characteristics, but the limiting characteristics, when the nonlinear asymmetry is high. Figure 10 shows the limiting characteristics of the high nonlinear asymmetry coupler. Obviously, the high nonlinear asymmetry coupler can be used as an optical limiter not for switching.

3 Conclusion

The nonlinear coupler with arbitrary linear and nonlinear mismatch is examined. Analytical solutions for the single-input

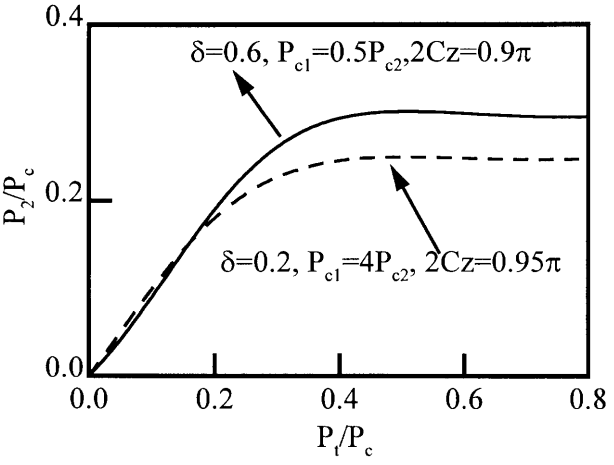

Fig. 10. Limiting characteristics for the high nonlinear asymmetry coupler, where all the power is launched into waveguide 1

asymmetrical mismatch nonlinear coupler are presented in a simple form. Based on these solutions, the general conditions for complete power in a coupler are also presented analytically. Based on this feature the coupler can be used as a power filter (see Fig. 9). In addition, we also show that the electro-optical switch with ultralow switching-voltage is possible. The equations for solving the conditions associated with the equilibrium state are suggested. Without solving differential equations, the input conditions associated with the stable and unstable equilibrium are also present in the case of single-input cases. We also show that there is only one or a pair of trajectories in the portrait when the two constants of the nonlinear system are given. It makes the analysis of the nonlinear coupler by means of the portrait simpler. Interestingly, the high asymmetrical coupler can be used as an all-optical limiter but not as a switch.

References

1. S.M. Jensen: IEEE J. Quantum Electron. **QE-18**, 1580 (1981)
2. A.T. Pham, L.N. Binh: J. Opt. Soc. Am. B **8**, 1914 (1991)
3. K. Kitayama, S. Wang: Appl. Phys. Lett. **43**, 17 (1983)
4. Y. Chen, A.W. Snyder, D.J. Mitchell: Electron. Lett. **26**, 77 (1990)
5. Y. Wang: J. Lightwave Tech. **17**, 292 (1999)
6. Y. Wang, J. Liu: IEEE Photon. Tech. Lett. **11**, 72 (1999)
7. Carsten, Thirstrup: IEEE J. Quantum Electron. **31**, 2101 (1995)
8. S.R. Friberg, Y. Silberberg, M.K. Oliver, M.J. Andrejco, M.A. Saifi, P.W. Smith: Appl. Phys. Lett. **51**, 135 (1987)
9. A. Villeneuve, C.C. Yang, P.G.J. Wigley, G.I. Stegeman, J.S. Aitchison, C.N. Ironside: Appl. Phys. Lett. **61**, 147 (1992)
10. J.S. Aitchison, A. Villeneuve, G.I. Stegeman: Opt. Lett. **20**, 698 (1995)
11. A.T. Pham, L.N. Binh: Int. J. Optoelectron. **5**, 367 (1990)
12. Y. Chen, A.W. Snyder, D.N. Payne: IEEE J. Quantum Electron. **28**, 239 (1992)
13. S. Wabnitz, E.M. Wright, C.T. Seaton, G.I. Stegeman: Appl. Phys. Lett. **49**, 838 (1986)
14. G.I. Stegeman, G.T. Seaton, C.N. Ironside, T. Cullen, A.C. Walker: Appl. Phys. Lett. **50**, 1037 (1987)
15. S. Trillo, S. Wabnitz: Appl. Phys. Lett. **49**, 752 (1986)
16. J. Atai, Y. Chen: IEEE J. Quantum Electron. **29**, 242 (1993)
17. Y. Kiyotoshi, M. Hiroshi, M. Naoto: J. Lightwave Tech. **14**, 628 (1996)
18. C.C. Yang, A.J.S. Wang: IEEE J. Quantum Electron. **28**, 479 (1992)
19. Y. Chen: Electron. Lett. **26**, 1374 (1990)
20. B. Daino, G. Gregori, S. Wabnitz: Opt. Lett. **11**, 42 (1986)
21. S. Trillo, S. Wabnitz, B. Daino: Ultrafast All-optical Switching in Optical Fibers, Nonlinear Optics and Optical Computing, ed. by S. Martellucci, A.N. Chester (Plenum Press, New York 1990) pp. 217–227
22. A.M. Weiner, Y. Silberberg, H. Fouckhardt, D.E. Leaird, M.A. Saifl, M.J. Andrejco, P.W. Smith: IEEE J. Quantum Electron. **25**, 2648 (1989)
23. G.P. Agrawal: *Nonlinear Fiber Optics* (Academic Press, Boston 1989)